journal

J. Am. Ceram. Soc., 98 [4] 1095–1098 (2015)
DOI: 10.1111/jace.13406

Uncovering Nanoclusters in Amorphous AlN: An *Ab Initio* Study

Murat Durandurdu†

Department of Materials Science & Nanotechnology Engineering, Abdullah Gül University, Kayseri 38039, Turkey

Amorphous AlN (*a*-AlN) is modeled by melt-and-quench technique using *ab initio* molecular dynamic simulations. For the first time, three-dimensional hexagonal-like nanoclusters embedded in amorphous matrix are proposed for *a*-AlN. The model is chemically ordered and dominantly fourfold coordinated, but its short-range order is partially different from the crystalline morphology due to the nanoclusters. The model is semiconducting with a theoretical band gap of 1.7 eV.

I. Introduction

Aluminum nitride (AlN), a technologically important electronic ceramic with a wide band gap of 6.2 eV,[1] possesses superior physical properties.[2–4] It has a high-melting point, high thermal conductivity, good dielectric strength and high hardness. Due to these remarkable physical natures, AlN is considered as a good candidate for a wide range of high technological applications such as microelectronic substrate applications, short wavelength light-emitting diodes, laser diodes, and optical detectors, as well as for high-temperature, high-power, and high-frequency devices.

At ambient conditions, AlN has two crystalline structures: the hexagonal wurtzite (WZ) crystal with space group $P6_3mc$ and the zinc blende (ZB) cubic crystal with the space group $F\bar{4}3m$. However, the ZB phase is stable only when it is very thin 1.5–2.0 nm and it transforms to the WZ structure at larger thickness.[5] In addition to these crystalline modifications, there exists amorphous form of AlN (*a*-AlN), which can be easily grown using reactive sputtering, plasma-enhanced atomic layer deposition, and single ion beam sputtering techniques.[6–12] *a*-AlN is expected to have some important technological applications[13] but regrettably, its fundamental physical properties are still not well understood because of the limited investigations on this material. To understand its basic physical properties, it is necessary to have an atomistic level description of *a*-AlN. Such a description can be easily achievable through the current simulation techniques. To our knowledge, there are a few theoretical works on *a*-AlN. The first simulation based on an empirical potential did focus on only mechanical and thermal properties of *a*-AlN but did not discuss its local structural arrangement in details.[14] The second one was a first-principles calculation and provided valuable information regarding the short-range order of *a*-AlN.[15] The third one is based upon an approximate *ab initio* calculation and offered substantial information about not only the structural parameters but also the electronic structure of *a*-AlN.[16] Both quantum mechanical simulations[15,16] strongly suggested that *a*-AlN is indeed chemically ordered, that is, no Al–Al or N–N bonds exist in their model. However, the striking difference between these two first-principles calculations is the coordination distributions. Although threefold coordination defects were observed in both amorphous networks, fivefold coordination defects were not presented in the model of Ref. [16]. The dissimilarity between these two simulations can be associated with many factors but two suspects that can be noticed effortlessly are the size of simulation boxes (64 atoms[15] vs 216 atoms[16]) and the simulation time (less than 1.0 ps[15] vs several ps[16]) used in these studies.

The realistic representation of structural and chemical defects in simulations for disordered systems is really important as they play a key role in their physical properties. Therefore, an additional study is mandatory to reveal the accurate microstructure of *a*-AlN and understand its physical properties. Here, we systematically explore the structural and electronic properties of *a*-AlN obtained from its liquid state using an *ab initio* molecular dynamics technique and uncover, for the first time, three-dimensional hexagonal-like nanoclusters embedded in the amorphous matrix. The formation of nanoclusters in *a*-AlN yields *partially* different local environments relative to the crystalline morphology even though the model is chemically ordered and dominantly fourfold coordinated. These findings will lead to new perspectives on *a*-AlN.

II. Method

The calculations were carried out using the SIESTA code.[17] The method is based on the density functional theory (DFT) adopting a localized linear combination of atomic orbital basis sets for the description of valence electrons and norm-conserving nonlocal pseudopotentials for atomic core. The pseudopotentials were constructed using Troullier and Martins scheme.[18] The exchange correlation energy was calculated using the generalized gradient approximation that implements Becke gradient exchange functional[19] and Lee, Yang, Parr correlation functional.[20] The double-ξ plus polarized orbitals were employed. A uniform mesh with a plane wave cutoff of 120 Ryd was used to represent the electron density, the local part of the pseudopotentials, and the Hartree and the exchange-correlation potential. The molecular dynamics (MD) simulations were performed using the NPT (constant number of atoms, constant pressure, and constant temperature) ensemble. The simulation cell consists of 216 atoms with periodic boundary conditions. We used Γ point sampling for the Brillouin zone integration. The initial ZB structure was melted at 5500 K for 1.0 ps. The liquid state was quickly cooled to 3000 K and then to 2600 K. At these temperatures the structure was equilibrated for 7.5 and 12 ps, respectively. The structure was cooled to 300 K in a period of 10 ps. The amorphous network at 300 K was finally relaxed. Each time step is one femtosecond (fs). Temperature was controlled using the velocity rescaling method. The volume of the supercell at zero pressure was equilibrated using the Parrinello Rahman technique.[21]

III. Results

To determine the interatomic correlations and the compare our model with the previously published models, we first

W.-Y. Ching—contributing editor

Manuscript No. 35573. Received September 11, 2014; approved November 24, 2014.
†Author to whom correspondence should be addressed. e-mail: murat.durandurdu@agu.edu.tr

study the total and partial pair distribution functions, which are presented in Fig. 1. The first sharp peak located at 1.91 Å in total pair distribution is due to the Al–N correlation. The second peak around 3.22 Å comes from both A–Al and N–N partial correlations. Although the first quantity is accord with the previous *ab initio* MD result of 1.91 Å (Ref. [15]), the second one is slight larger than 3.07 Å reported in that study.

We next focus on another essential structural parameter, coordination number. We use the Voronoi polyhedral technique to determine the coordination number. The computed coordination numbers, together with the earlier *ab initio* MD simulations' results are given in Table I. As seen from the table, the fourfold coordination is the most favorable unit in our amorphous model, similar to what has been observed in Refs. [15] and [16]. However, the amount of defects (threefold and fivefold) formed in our *a*-AlN system is noticeable less than the ones reported in those studies. So these findings might be interpreted as a tendency of our model to preserve more characteristic of crystalline morphology, relative to Refs. [15] and [16]. Based on the coordination distributions, it can be also concluded that the local structural arrangements obtained in these simulations (present and previous) are partially different from each other. The Voronoi examination further suggests that *a*-AlN is chemically ordered, that is, no Al–Al and N–N homopolar bonds exit in the model.

To have more information about the short-range order, we also analyze the model using three body correlations, bond-angle distribution functions. The Al–N–Al and N–Al–N distributions are illustrated in Fig. 2. In contrast to our anticipation (since the model has an average coordination of four), the model features very broad distributions with a main peak to close to the tetrahedral angle of 109.47° similar to what has been observed in Ref. [16]. The main peak is due to the ideal or distorted tetrahedral units in the model. On the other hand, the unexpected subpeaks around 88°–90° and large angles indicate some local structural arrangements, very different from the tetrahedral configurations. Similar subpeaks were indeed reported in different nitrogen based amorphous models such as GaN, $Al_xGa_{1-x}N$ and InN and attributed to the existence of the edge-sharing units, that is, the fourfold rings, which do not exist in their crystalline counterparts.[12,22,23] To determine the physical origin of these subpeaks in our model, we perform a ring statistic investigation and find quite amount of fourfold rings. A careful analysis of these units reveals that they are indeed responsible for the subpeaks and neighboring angles as suggested in the previous simulations. The large angles >130°

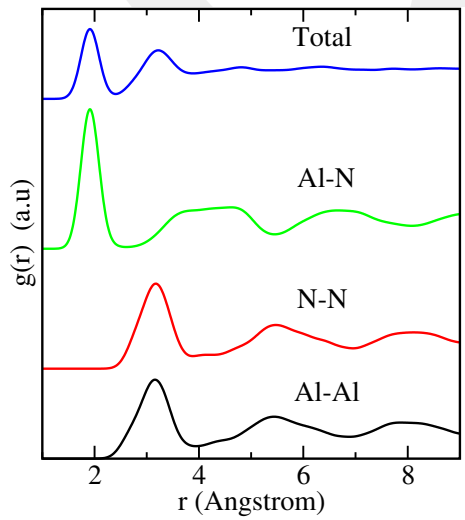

Fig. 1. Total and partial pair distribution functions.

Table I. Coordination Distribution of *a*-AlN

Threefold (%)	Fourfold (%)	Fivefold (%)	Ref.
4.6	91.7	3.7	Present study
22	78	0	[16]
13	81	6	[15]

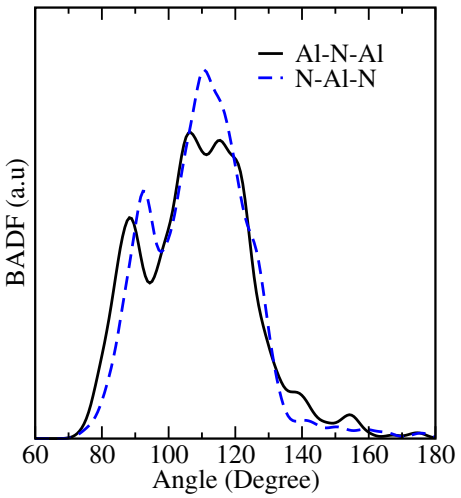

Fig. 2. Al–N–Al and N–Al–N bond angle distributions.

are due to the fivefold-coordinated atoms and their fourfold-coordinated neighboring atoms having edge-sharing units. Another interesting observation is the formation of slightly deformed hexagons with the sixfold rings as seen in AlN nanosheet.[24] The hexagons produce angles around 120°. In some parts of the model, two close hexagons are linked each other by bonds and form three-dimensional hexagonal-like nanoclusters (drumlike) having the fourfold and sixfold rings as shown in Fig. 3. It should be emphasized here that these nanoclusters have one or two missing bonds and hence they are uncompleted and distorted, which is probably results of the disorder nature of model. Consequently, they have non-uniform bond lengths and angles. The Al–N bonds range from 1.86 to 2.1 Å and the angles (Al–N–Al or N–Al–N) range from 75° to 130°. The bond separations are close to the Al–N bond distances of 1.85—197 Å formed in Al_6N_6 hexagonal cluster.[25] These findings are particularly important because they propose, for the first time, the existence of hexagons and hexagonal-like nanoclusters embedded in the amorphous matrix in AlN. Our results further suggest that *a*-AlN has partially different local structural arrangements relative to the crystalline phases due to the nanoclusters.

It should be noted here that these types of clusters are not a novel structure for AlN. To date a wide ranges of AlN-based nanostructures have been successfully synthesized using different experimental procedures. A graphite-like hexagonal AlN nanosheet is known to exist[24] and hexagon and three-dimensional hexagonal (drumlike) clusters were found to be the lowest energy isomers for $(AlN)_n$ ($n = 3$ and 6) (Refs. [25] and [26]). Therefore, their formation in *a*-AlN cannot be questionable but really thrilling because it might lead to a new research direction in AlN. If the size of clusters is controlled experimentally, then the physical properties of *a*-AlN can be tunable to desirable values and hence it can find a wide variety of new technological applications.

Regrettably, we are not able to provide full supportive results to neither of the previous simulations.[15,16] Indeed our simulations suggest a more complex structure for *a*-AlN relative to them. So one might ask the physical origin of these different observations, in particular the formation of nanoclusters. In Ref. [15] the size of the simulation box is too small

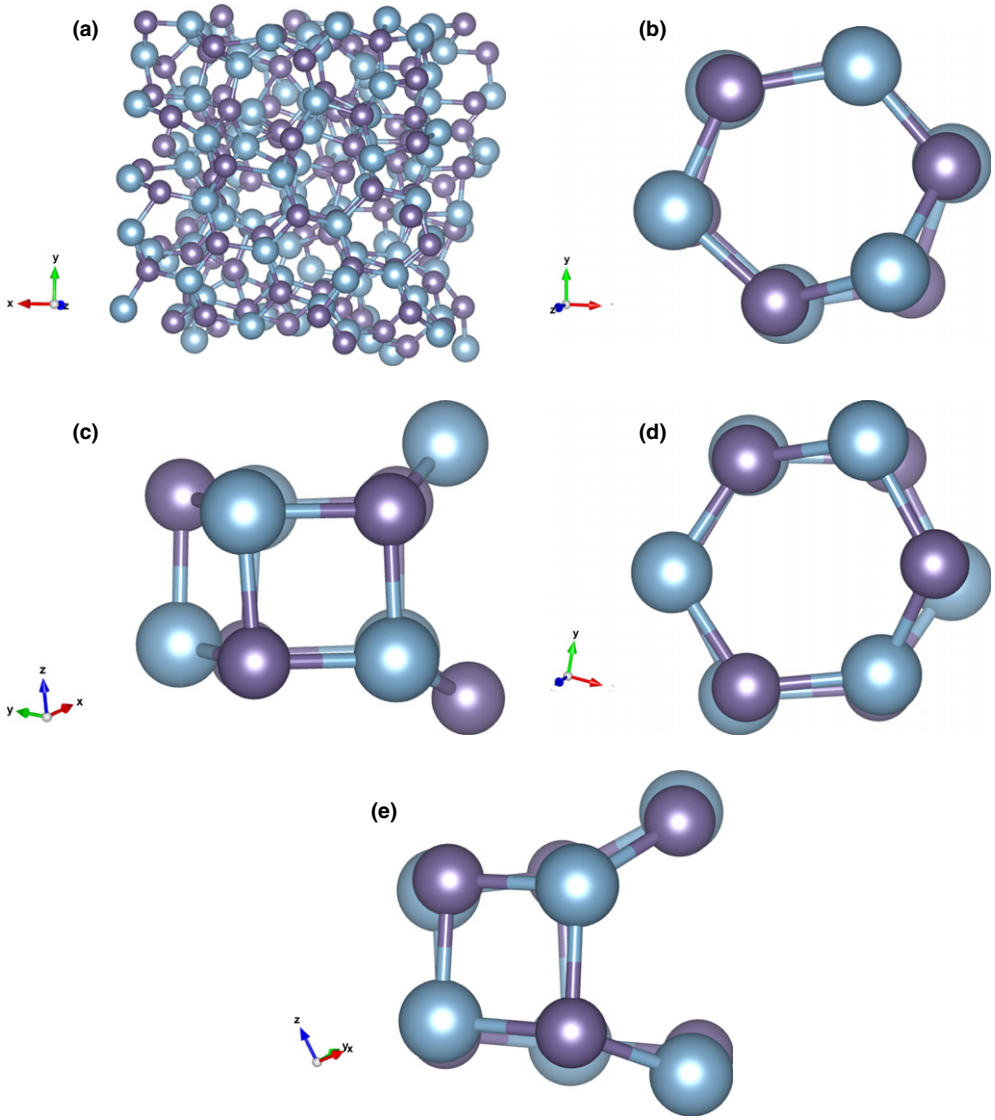

Fig. 3. (a) *a*-AlN model. (b) and (c) Hexagonal-like nanoclusters with missing one bond. (d) and (e) Hexagonal-like nanoclusters with missing two bonds.

and the time scale is too short to capture such features in *a*-AlN. In Ref. [16], even though the size is big enough, the total simulation time is quite shorter than what has been used in our simulation. In addition, the simulation technique used in Ref. [15] has some limitations.[22] Therefore, the dissimilar results can be attributed to the size of the simulation boxes, the timescale of simulations and the parameters (basis, exchange correlation functional, etc.) used in these simulations.

Finally we study the electronic property of *a*-AlN, described by electronic density of state and compare it with that of wurtzite AlN (72 atoms model). The computed EDOS for amorphous and crystalline phases near the Fermi level located at $E = 0$ eV is shown in Fig. 4. The GGA band gap as a difference between the top of the valence band and the bottom of the conduction band is about 4.0 eV for the crystal, which is accord with the previous DFT calculations[27] but as expected it is smaller than experimental result of 6.2 eV (Ref. [1]), mainly because of the well-known shortcoming of DFT within the GGA in describing excited states. The band gap obtained from the present calculation is not therefore comparable with the experiment results but give some idea about relative band gap difference between two states of AlN. As seen from the Fig. 4, for *a*-AlN, the top of the valance states and the bottom of the conduction states move toward to the Fermi level, resulting in a closure of its

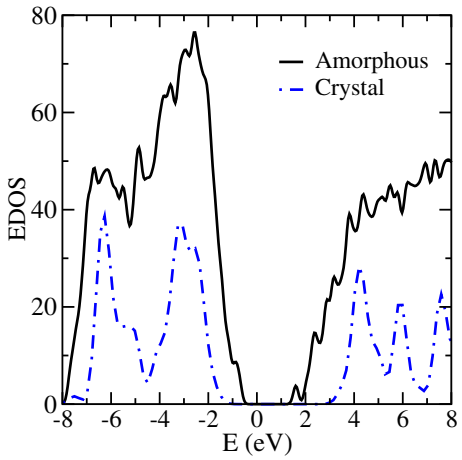

Fig. 4. Electron density of states of amorphous and crystalline AlN near the Fermi level.

band gap energy. The theoretical bad gap for *a*-AlN is calculated to be 1.7 eV. Based on compression of these values, the experimental gap energy for *a*-AlN can be estimated around

2.6 eV. Note that amorphous systems do not have unique structure in a contrast to crystals and thus they can have a slightly different topology (depending on preparation techniques) and band gap energy. As the band gap energy correlates with the size of the clusters, *a*-AlN can serve as a good candidate for gap engineering if the size of clusters can be changed easily.

IV. Conclusions

In summary, we have generated an *a*-AlN model by quenching from the melt and found that *a*-AlN has a tendency to form a chemically ordered topology with an average coordination of four. However, the model has partially different local structure than crystalline phases because of the hidden hexagonal-like nanoclusters in amorphous matrix. Uncovering nanoclusters probably will lead to more future works on *a*-AlN since its properties can be engineered to desirable values by altering the size of these clusters. It should be noted here that we certainly have finite size artifacts in our simulation, which might artificially favor an amorphous model with no chemical disorder. A small/negligible amount of homopolar bonds might be presented in a larger model or in experimentally prepared samples. In addition, the size of nanoclusters can correlate with the size of the simulation box and hence the nanoclusters might be at a larger scale for a bigger model. Of course any structural change influences on the electronic properties of *a*-AlN. Finally, we would like to remark on unexpected structural parameters such as fourfold rings, edge-sharing units, etc., reported for other nitrogen based amorphous materials,[16,22,23] similar to those found in *a*-AlN. On the basis of those reports, we are, however, not able to propose three-dimensional nanoclusters (nanocages) for them because each material appears to have different favorable cluster configurations,[25] different from those of AlN. However, further experimental and theoretical studies are needed to investigate their microstructures in details.

Acknowledgment

This work was supported by the Scientific and Technical Research Council of Turkey (TÜBİTAK) under BİDEB-2232 program.

References

[1]L. I. Berger, *Semiconductor Materials*, p. 124. CRC Press, New York, NY, 1997.

[2]A. W. Weimer, G. A. Cochran, G. A. Eisman, J. P. Henley, B. D. Hook, L. K. Mills, T. A. Guiton, A. K. Knudsen, N. R. Nicholas, J. E. Volmering, and W. G. Moor, "Rapid Process for Manufacturing Aluminum Nitride Powder," *J. Am. Ceram. Soc.*, **77**, 3–18 (1994).

[3]A. V. Virkar, T. B. Jackson, and R. A. Cutler, "Thermodynamic and Kinetic Effects of Oxygen Removal on the Thermal Conductivity of Aluminum Nitride," *J. Am. Ceram. Soc.*, **72**, 2031–42 (1989).

[4]J. H. Edgar (Ed.), *Properties of Group-III Nitrides*, EMIS Data Reviews Series. IEE, London, 1994.

[5]I. Petrov, E. Mojab, R. C. Powell, J. E. Greene, L. Hultman, and J. E. Sundgren, "Synthesis of Metastable Epitaxial Zincblende-Structure AlN by Solid-State Reaction," *Appl. Phys. Lett.*, **60**, 2491–3 (1992).

[6]H. Chen, K. Chen, D. A. Drabold, and M. E. Kordesch, "Band Gap Engineering in Amorphous AlGaN Alloys: Experiments and *Ab Initio* Calculations," *App. Phys. Lett.*, **77**, 1117–9 (2000).

[7]J. M. Khoshman and M. E. Kordesch, "Spectroscopic Ellipsometry Characterization of Amorphous Aluminum Nitride and Indium Nitride Thin Films," *Phys. Status Solidi (c)*, **2**, 2821–7 (2005).

[8]J. M. Khoshman and M. E. Kordesch, "Optical Characterization of Sputtered Amorphous Aluminum Nitride Thin Films," *J. Non-Cryst. Solids*, **351**, 3334–40 (2005).

[9]M. Maqbool and T. R. Corn, "Optical Spectroscopy and Energy Transfer in Amorphous AlN-Doped Erbium and Ytterbium Ions for Applications in Laser Cavities," *Opt. Lett.*, **35**, 3117–9 (2010).

[10]M. Bosund, T. Sajavaara, M. Laitinen, T. Huhtio, M. Putkonen, V. M. Airaksinen, and H. Lipsanen, "Properties of AlN Grown by Plasma Enhanced Atomic Layer Deposition.," *Appl. Surf. Sci.*, **257**, 7827–30 (2011).

[11]F. Hajakbari, M. M. Larijani, M. Ghoranneviss, M. Aslaninejad, and A. Hojabri, "Optical Properties of Amorphous AlN Thin Films on Glass and Silicon Substrates Grown by Single Ion Beam Sputtering.," *Jpn. J. of Appl. Phys.*, **49**, 095802–7 (2010).

[12]F. Jose, R. Ramaseshan, S. Dash, S. Bera, A. K. Tyagi, and B. Raj, "Response of Magnetron Sputtered AlN Films to Controlled Atmosphere Annealing," *J. Phys. D: Appl. Phys.*, **43**, 075304, 10pp (2010).

[13]J. M. Khoshman, Spectroscopic Ellipsometry Characterization of Single and Multilayer Aluminum Nitride/Indium Nitride Thin Film Systems, Ph.D. Thesis. Ohio University, Athens, OH, 2005.

[14]P. Vashishta, R. K. Kalia, A. Nakano, and J. P. Rino, and Collaboratory for Advanced Computing and Simulations, "Interaction Potential for Aluminum Nitride: A Molecular Dynamics Study of Mechanical and Thermal Properties of Crystalline and Amorphous Aluminum Nitride," *J. App. Phys.*, **109**, 033514–0335211 (2011).

[15]D. G. McCulloch, D. R. McKenzie, and C. M. Goringe, "*Ab Initio* Study of Structure in Boron Nitride, Aluminum Nitride and Mixed Aluminum Boron Nitride Amorphous Alloys," *J. App. Phys*, **88**, 5028–33 (2000).

[16]K. Chen and D. A. Drabold, "First Principles Molecular Dynamics Study of Amorphous $Al_xGa_{1-x}N$ Alloys," *J. App. Phys*, **91**, 9743–51 (2002).

[17]P. Ordejón, E. Artacho, and J. M. Soler, "Self-Consistent Order-N Density- Functional Calculations for Very Large Systems," *Phys. Rev. B*, **53**, 10441–4 (1996).

[18]N. Troullier and J. M. Martins, "Efficient Pseudopotentials for Plane-Wave Calculations," *Phys. Rev. B*, **43**, 1993–2006 (1991).

[19]A. D. Becke, "Density-Functional Exchange Energy Approximation with Correct Asymptotic Behavior," *Phys. Rev. A*, **38**, 3098–100 (1988).

[20]C. Lee, W. Yang, and R. G. Parr, "Development of the Colle-Salvetti Correlation-Energy Formula into a Functional of the Electron Density," *Phys. Rev. B*, **37**, 785–9 (1988).

[21]M. Parrinello and A. Rahman, "Polymorphic Transitions in Single Crystals: A New Molecular Dynamics Method," *J. Appl. Phys.*, **52**, 7182–90 (1981).

[22]B. Cai and D. A. Drabold, "Properties of Amorphous GaN from First-Principles Simulations," *Phys. Rev. B*, **84**, 075216–21 (2011).

[23]B. Cai and D. A. Drabold, "*Ab Initio* Models of Amorphous InN," *Phys. Rev. B*, **84**, 195204–7 (2009).

[24]P. Tsipas, S. Kassavetis, D. Tsoutsou, E. Xenogiannopoulou, E. Golias, S. A. Giamini, C. Grazianetti,, D. Chiappe, A. Molle, M. Fanciulli, and A. Dimoulas, "Evidence for Graphite-Like Hexagonal AlN Nano Sheets Epitaxially Grown on Single Crystal Ag(111)," *Appl. Phys. Lett.*, **103**, 251605–7 (2013).

[25]A. Costales, A. K. Kandalam, and R. Pandey, "Theoretical Study of Neutral and Anionic Group III Nitride Clusters: M*n*N*n*(M)Al, Ga,and In; $n = 4$-6)," *J. Phys. Chem. B*, **107**, 4508–14 (2003).

[26]A. Costales, M. A. Blanco, E. Francisco, R. Pandey, and A. M. Pendás, "Evolution of the Properties of Al*n*N*n* Clusters with Size," *J. Phys. Chem. B*, **109**, 24352–60 (2005).

[27]Z. Dridi, B. Bouhafs, and P. Ruterana, "Pressure Dependence of Energy Band Gaps for $Al_xGa_{1-x}N$, $In_xGa_{1-x}N$ and $In_xAl_{1-x}N$," *New J. Phys.*, **4**, 1–15 (2002). □